Turbidity-free fluorescence spectroscopy of biological tissue

4 authors, including:

Qingguo Zhang
Lanzhou University
201 PUBLICATIONS   **3,316** CITATIONS

SEE PROFILE

Markus G Müller
Massachusetts Institute of Technology
19 PUBLICATIONS   **2,632** CITATIONS

SEE PROFILE

Turbidity-free fluorescence spectroscopy of biological tissue

Qingguo Zhang, Markus G. Müller, Jun Wu, and Michael S. Feld

*Laser Biomedical Research Center, G. R. Harrison Spectroscopy Laboratory, Massachusetts Institute of Technology,
Cambridge, Massachusetts 02139*

We present a method based on photon migration of extracting intrinsic fluorescence spectra from turbid media,
using concomitantly measured fluorescence and reflectance.   Intrinsic fluorescence is defined as fluorescence
that is due only to fluorophores, without interference from the absorbers and scatterers that are present.
Application to fluorescence spectra taken with tissue phantoms and human mucosal tissues demonstrates
excellent agreement in both spectral line shape and intensity between the extracted and the directly measured
intrinsic fluorescence spectra.   © 2000 Optical Society of America
    OCIS codes: 170.3660, 170.6510, 170.4580, 170.7050.

Fluorescence from human tissue and from exogenous dyes injected into the body has been widely used for diagnosing[1] and treating[2] disease. Biological tissues are turbid media in which the predominance of light scattering unavoidably entangles the effects of absorption and fluorescence. The interplay of absorption and scattering can substantially distort the measured fluorescence. Therefore it is important to have a method of extracting the intrinsic fluorescence from the measured tissue fluorescence. Here intrinsic fluorescence is defined as the fluorescence that is due only to fluorophores, without interference from the absorbers and scatterers that are present in the tissue. Knowledge of the intrinsic fluorescence permits unambiguous interpretation of the information about the tissue fluorophores.

Beginning with the pioneering work of Mayevsky and Chance,[1] ideas for using information contained in reflectance spectra to remove the effects of scattering and absorption from tissue fluorescence[2-5] and correcting the measured fluorescence to eliminate artifacts from absorption have been advanced. Although some of these studies demonstrated good agreement between theoretically extracted and experimentally measured intrinsic fluorescence spectra, the analyses have been limited mostly to light-delivery–collection geometries of infinite extent and to visible wavelengths longer than 500 nm. Thus information provided at shorter wavelengths by important tissue fluorophores was excluded. We note that the greatest distortion of fluorescence spectra occurs for emission near 420 nm, where hemoglobin absorbs strongly. Removal of such distortion is particularly important for ultraviolet excitation wavelengths, which have been shown to contain important diagnostic information. In addition, optical fiber probes collect clinical fluorescence spectra over only a small spot (~1 mm in diameter), rendering the assumption of an infinite light-delivery–collection geometry invalid. Because of these limitations, to our knowledge intrinsic fluorescence spectra have not yet been correctly extracted from clinically obtained spectra.

In this Letter we present a method based on photon migration of reliably extracting intrinsic fluorescence from clinical tissue fluorescence and reflectance spectra collected concomitantly. Our approach is based on the fact that, when reflectance and fluorescence are collected from a given tissue site with the same probe, absorption and scattering distort fluorescence and reflectance spectra similarly, because the diffusely reflected and the fluorescence photons traverse similar paths.

Our method is a modification of a model proposed by Wu *et al.*[4] Because of the approximations made, the applicability of that model was limited to the case of small hemoglobin absorption, and hence to wavelengths above 500 nm. Here we refine that model and demonstrate the applicability of the resulting algorithm to a wide emission range, 370–700 nm, which encompasses the prominent visible absorption features of hemoglobin.

In photon migration theory, light propagation in a turbid medium is described by photons traveling in paths with discrete nodes, at which absorption, scattering, and fluorescence events occur. Let ρ_n be the probability that a photon will enter the medium, undergo n scattering events, escape from the medium, and finally be collected by a probe. According to Wu *et al.*[2], ρ_n can be approximated as an exponential function of n, $\rho_n \approx \kappa \exp(-\beta n)$, where κ and β are parameters that are independent of the number of steps n but dependent on the scattering properties of the medium (see below). Let μ_a and μ_s be the absorption and the scattering coefficients, respectively, of the turbid medium. The albedo, $a = \mu_s/(\mu_a + \mu_s)$, then represents the fraction of photons that are not absorbed during each interaction event and thus can be considered the photon weight reduction factor for that event. The reflectance R of a homogeneous medium of scatterers and absorbers can then be modeled as

$$R = \sum_{n=1}^{\infty} a^n \rho_n = \frac{\kappa a \exp(-\beta)}{1 - a \exp(-\beta)}. \qquad (1)$$

Let R_0 be the reflectance in the absence of absorption (i.e., $a = 1$), and let $\epsilon = \exp \beta - 1$. Note that $R_0 \to 1$ when the collection size of the probe is infinite; otherwise, $R_0 < 1$ and is generally wavelength dependent. From Eq. (1), we have $\kappa = \epsilon R_0$ and, according to Wu *et al.*[2], $\beta = S(1 - g)$, where S is a probe-specific constant and g is the anisotropy parameter of the medium.[6] A related expression was given in Ref. 2, in which the sum was approximated by an integral. This expression is valid only for $a \approx 1$ and is insufficient for modeling fluorescence when

absorption is strong. Thus the use of the right-hand form of Eq. (1) is essential.

We now consider a single fluorophore in a homogeneous turbid medium and assume that absorption of the fluorescence photons does not result in secondary emission, as is the usual case in biological tissue. Let μ_f be the absorption coefficient of the fluorophore and ϕ_{xm} be its fluorescence quantum yield, in which the subscripts x and m denote evaluation of the corresponding quantities at excitation frequency ν_x and emission frequency ν_m. Consider a fluorescence path in the medium that consists of n scattering events (nodes) in which the fluorescence occurs at the $(i + 1)$th node. Let ρ_{ni} denote the fluorescence escape probability for this path. Extending escape probability ρ_n for the reflectance path, we assume that $\rho_{ni} = \sqrt{\kappa_x \kappa_m} \exp[-\beta_x(i + 1) - \beta_m(n - i - 1)]$. The fluorescence intensity of the medium can then be modeled as

$$F_{xm} = \frac{I_x}{h\nu_x} \left[\sum_{n=1}^{\infty} \sum_{i=0}^{n-1} \rho_{ni} a_x^i \left(\frac{\mu_{fx}}{\mu_{ax} + \mu_{sx}} \phi_{xm} \right) a_m^{n-i-1} \right] h\nu_m,$$

(2)

where I_x denotes the excitation intensity. Consequently, the expression in brackets has the meaning of fluorescence photons per excitation photon. After the photon transverses the first i absorption–scattering nodes and experiences propagation loss, its weight becomes a_x^i for each incident excitation photon. For each excitation photon arriving at the $(i + 1)$th node, $\mu_{fx}/(\mu_{ax} + \mu_{sx})$ photons will be absorbed by the fluorophore. For each photon absorbed by the fluorophore, ϕ_{xm} fluorescence photons will be generated. The propagation loss of the fluorescence photons is accounted for by the factor a_m^{n-i-1}.

For a dilute, optically thin ($\mu_{fx}l \ll 1$) sample of thickness l, with the same amount of fluorophore but without other absorbers and scatterers, one obtains the intrinsic fluorescence,

$$f_{xm} = (I_x/h\nu_x)\mu_{fx}l\phi_{xm}h\nu_m. \qquad (3)$$

The fluorescence expression in Eq. (2) can be expressed in terms of reflectance with the help of Eq. (1). We can then combine the result with Eq. (3) to obtain the relationship among intrinsic fluorescence spectrum f_{xm}, experimentally measured fluorescence spectrum F_{xm}, and reflectance spectrum R_m:

$$f_{xm} = \frac{F_{xm}}{\dfrac{1}{\mu_{sx}l} \left(\dfrac{R_{0x}R_{0m}}{\epsilon_x \epsilon_m} \right)^{1/2} \dfrac{R_x}{R_{0x}} \left(\dfrac{R_m}{R_{0m}} + \epsilon_m \right)} . \qquad (4)$$

Equation (4) should hold for a probe of arbitrary delivery–collection geometry, as long as the fluorescence and reflectance are measured with the same probe; note that R_0 is a function of wavelength. Note that Eq. (4) can be used to extract an intrinsic fluorescence excitation–emission matrix (EEM) from an experimentally measured fluorescence EEM. When the medium contains multiple fluorophores, one need

only replace every occurrence of $\mu_{fx}\phi_{xm}$ in Eqs. (2) and (3) with a summation of this quantity over all fluorophores. Doing so will result in the same expression as in Eq. (4).

To test the effectiveness of Eq. (4) in extracting intrinsic fluorescence we conducted a preliminary experimental study, using tissue phantoms as well as *ex vivo* and *in vivo* human tissues. All reflectance and fluorescence data were recorded simultaneously with the FastEEM instrument.[7] The tissue phantoms were suspensions of polystyrene beads (1-μm diameter; Polyscience) in aqueous solutions of furan 2 (Lambdachrome) and hemoglobin (Sigma). Figure 1 presents the fluorescence spectrum of a representative tissue phantom and the experimentally measured intrinsic fluorescence spectrum excited at 337 nm. The intrinsic fluorescence spectrum was obtained from dilute aqueous solutions of pure furan 2 (0.9 μM). The distortion that is due to the interplay of absorption of oxyhemoglobin at ~415 nm and scattering of the beads can be readily seen in the phantom fluorescence spectrum.

To use Eq. (4) for intrinsic fluorescence extraction we need to compute the quantities in Eq. (4) that are unavailable experimentally. The absorption coefficient μ_a of the phantoms was varied from 0 to 5 mm^{-1} and could be calculated with the experimental hemoglobin concentrations and the well-documented values of the extinction coefficients of hemoglobin. Using Mie scattering theory,[6] we can calculate μ_s and g for the phantoms, since the diameter, concentration, and refractive index of the beads are known. Measured fluorescence and reflectance spectra were used for F_{xm} and R_m in Eq. (4). Other reflectances in Eq. (4), R_x, R_{0x}, and R_{0m}, were calculated by analytical extension of the diffuse reflectance model $R(\mu_a, \mu_s, g)$ [e.g., $R_{0x} = R(0, \mu_{sx}, g_x)$] of Zonios *et al.*[8] The probe-specific parameters S and l were determined once with a calibration phantom and kept unchanged for the remaining phantoms and tissue samples. With this
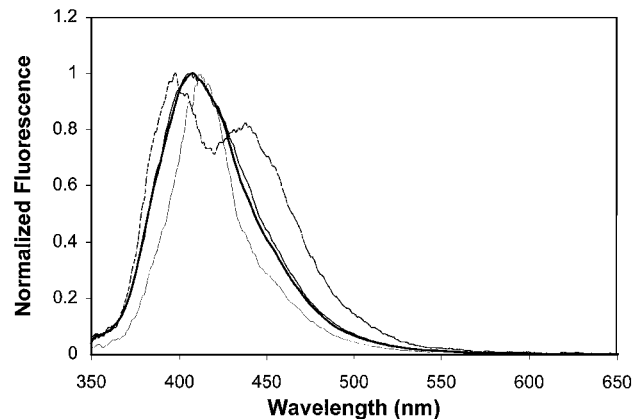

Fig. 1. Fluorescence spectra of a tissue phantom. The phantom is an aqueous solution–suspension of hemoglobin (2 g/l), polystyrene beads (0.65% by volume), and furan 2 (0.9 μM). All spectra were excited with $\lambda_x = 337$ nm. – – – –, measured phantom fluorescence; ...., intrinsic fluorescence of pure furan 2; ——, modeled intrinsic fluorescence from Eq. (4); ——, modeled intrinsic fluorescence from Ref. 2.
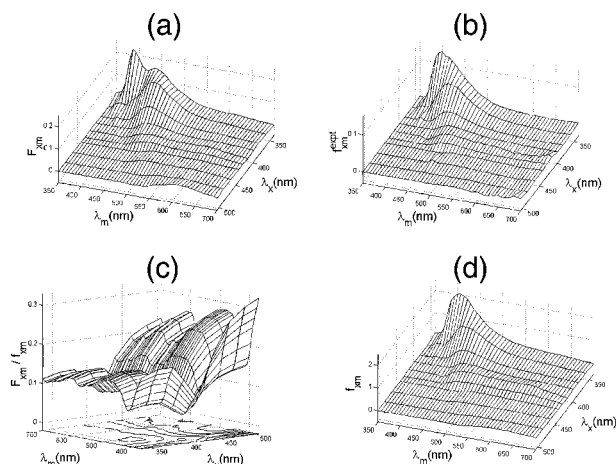
Fig. 2. Fluorescence EEM spectra of minced tissue: (a) fluorescence EEM of the mince (several millimeters thick); (b) intrinsic fluorescence EEM of the mince, measured with a thin ($\sim$10-μm) section; (c) computed intrinsic fluorescence correction factor, F_{xm}/f_{xm}; (d) modeled intrinsic fluorescence EEM of the mince extracted from (a).
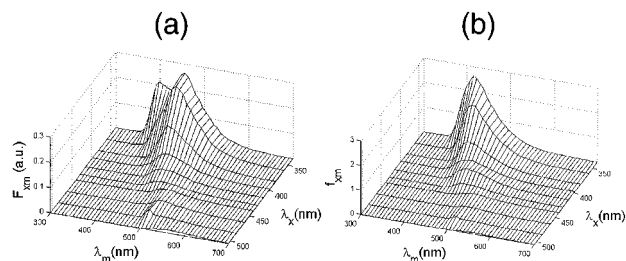

Fig. 3. Fluorescence EEM's of gastric mucosal tissue: (a) *in vivo* EEM spectra from a patient undergoing routine endoscopic examination, (b) extracted intrinsic fluorescence EEM spectra from (a).

information, the intrinsic fluorescence spectrum of the dye could be calculated. As can be seen from Fig. 1, there is excellent agreement with the experimentally measured intrinsic fluorescence spectrum. Good agreement was obtained for tissue phantoms with different hemoglobin concentrations.

We applied the algorithm, Eq. (4), to the FastEEM spectra of a minced sample of normal buccal mucosal tissue from a cadaver. The epithelium and submucosa were separated from the bulk tissue specimen and frozen with liquid nitrogen. We then minced the tissue in its frozen state to create a homogeneous distribution of endogenous tissue absorbers and fluorophores. We measured the intrinsic fluorescence of the minced tissue experimentally by obtaining the fluorescence spectra of a very thin ($\sim$10-μm) slice of the minced tissue.

The absorption and scattering parameters of the minced tissue were not known *a priori*. To obtain μ_a, μ_s, and g, we used an analytical model of $R(\mu_a, \mu_s, g)$ presented in Ref. 8 to fit the measured reflectance spectrum. The quantities in Eq. (4) that are unobtainable experimentally, R_{0x}, R_{0m}, ϵ, and ϵ_m, were then calculated by analytical extension of the reflectance model, as discussed above. Figures 2(a)

and 2(b) present the experimentally measured EEM's of the thick and the thin minced samples, respectively. Figure 2(c) shows the intrinsic fluorescence correction factor that was used to obtain the predicted intrinsic fluorescence EEM shown in Fig. 2(d). Very good agreement between the extracted [Fig. 2(d)] and the measured [Fig. 2(b)] intrinsic fluorescence EEM's can be seen. The ability to reconstruct intrinsic fluorescence EEM's demonstrates that the extraction method can recover not only spectral shape but also the intensity information of the intrinsic fluorescence and can therefore be used clinically.

To demonstrate the power of this extraction method we consider Fig. 3(a), a clinical fluorescence EEM from the gastric mucosa, which was obtained along with the reflectance spectrum (not shown) during upper GI endoscopy with an optical fiber probe. For $\lambda_x = 337$ nm we obtained two emission peaks, which might be interpreted as arising from two fluorophores. However, in the intrinsic fluorescence EEM, which we extracted using the above algorithm [Eq. (4)], there is only a single peak [Fig. 3(b)], indicating that the spectral structure is a distortion owing to the interplay of (hemoglobin) absorption and scattering. This result clearly underscores the advantage of working with the distortion-free intrinsic fluorescence, which directly provides biochemical information. We are successfully using such intrinsic fluorescence EEM's, extracted from clinical data, to obtain detailed information about the microscopic histochemical changes that accompany the onset of dysplasia, hypoxia, and other tissue abnormalities. We found that the resulting features correlate better with histologic tissue classifications than do those of the unprocessed spectra. This extraction method may also be applicable to other tissue spectroscopy techniques, such as Raman scattering.

References

1. A. Mayevsky and B. Chance, Science **217,** 537 (1982).
2. J. Wu, M. S. Feld, and R. P. Rava, Appl. Opt. **32,** 3585 (1993).
3. A. J. Durkin, S. Jaikumar, N. Ramanujam, and R. Richards-Kortum, Appl. Opt. **33,** 414 (1994).
4. C. M. Gardner, S. L. Jacques, and A. J. Welch, Appl. Opt. **35,** 1780 (1996).
5. N. N. Zhadin and R. R. Alfano, J. Biomed. Opt. **3,** 171 (1998).
6. A. Ishimaru, *Wave Propagation and Scattering in Random Media* (Academic, Orlando, Fla., 1978).
7. R. A. Zangaro, L. Silveira, Jr., R. Manoharan, G. Zonios, I. Itzkan, R. R. Dasari, J. Van Dam, and M. S. Feld, Appl. Opt. **35,** 5211 (1996).
8. G. Zonios, L. T. Perelman, V. Backman, R. Manoharan, M. Fitzmaurice, J. Van Dam, and M. S. Feld, Appl. Opt. **38,** 6628 (1999).